Journal of Cell Science 107, 517-526 (1994)
Printed in Great Britain © The Company of Biologists Limited 1994
JCS9090

Lamellipod extension and K^+ current in osteoclasts are regulated by different types of G proteins

Stuart A. Arkett[1,*], S. Jeffrey Dixon[1,2] and Stephen M. Sims[1]

[1]Department of Physiology, [2]Division of Oral Biology, The University of Western Ontario, London, Ontario, Canada N6A 5C1

*Author for correspondence

SUMMARY

Osteoclasts are the cells responsible for the resorption of bone and other mineralized tissues. GTP-binding proteins (G proteins) play important roles in regulating the activity of many cell types; however, there is limited knowledge of their functions in osteoclasts. We used the patch-clamp technique in the whole-cell configuration to introduce either hydrolysis-resistant guanosine triphosphate analogues or fluoroaluminate into single rat osteoclasts, and examined the effects of G protein activation on cell morphology and ionic conductances. Guanosine 5′-*O*-(3-thiotriphosphate) or 5′-guanylyl-imidodiphosphate, but not the control compounds adenosine 5′-*O*-(3-thiotriphosphate) or guanosine 5′-*O*-(2-thiodiphosphate), induced: (1) prompt spreading due to extension of lamellipodia; and (2) after a latency of several minutes, complete suppression of the inwardly rectifying K^+ current. Pertussis toxin did not alter either spreading or suppression of K^+ current induced by guanosine 5′-*O*-(3-thiotriphosphate). Cytochalasin D, but not colchicine, prevented guanosine 5′-*O*-(3-thiotriphosphate)-induced spreading, consistent with actin polymerization underlying lamellipod extension. Whole-cell capacitance did not change during guanosine 5′-*O*-(3-thiotriphosphate)-induced spreading, which is consistent with a lack of change in total plasma membrane area. Fluoroaluminate did not induce spreading, but it did suppress the K^+ current. The differential effects of fluoroaluminate and guanosine 5′-*O*-(3-thiotriphosphate) suggest that lamellipod extension is regulated by a small molecular mass, monomeric G protein, whereas the inwardly rectifying K^+ current is regulated by a large molecular mass, heterotrimeric G protein. Thus, osteoclast motility and ion transport are regulated by separate G protein-coupled pathways.

Key words: G protein, K^+ channel, pseudopod, bone resorption, motility

INTRODUCTION

GTP-binding proteins (G proteins) are involved in the transduction of signals from a variety of receptors to effectors, such as cytoskeletal elements, ion channels and enzymes (Neer and Clapham, 1988; Yatani et al., 1990; Hall, 1992). In this way, many hormones and neurotransmitters exert their effects on cell function. For example, several hormones and cytokines that affect bone remodelling operate through G protein-coupled pathways. The inhibitory actions of calcitonin on osteoclasts are thought to be mediated by two G proteins - one activating adenylyl cyclase and the other activating phospholipase C (Nicholson et al., 1986; Murrills and Dempster, 1990; Zaidi et al., 1990; Chabre et al., 1992). Platelet-activating factor, which in other systems is known to act through a G protein-coupled receptor (Venable et al., 1993), elevates cytosolic Ca^{2+} concentration in osteoclasts (Wood et al., 1991) and stimulates resorption (Zheng et al., 1993). Thus, G proteins appear to play important roles in the regulation of osteoclast activity, yet there is limited knowledge of the elements involved in the signalling pathways.

Osteoclasts alternate between motile and resorptive phases of activity (Kanehisa and Heersche, 1988), both of which are necessary for effective bone remodelling. The motile phase is characterized by lamellipod extension and retraction. During the resorptive phase, osteoclasts form a specialized seal with the substrate and acidify the resorption lacuna, leading to dissolution of bone mineral (Blair and Schlesinger, 1992). We have recently shown that rat osteoclasts express two phenotypes (‘rounded’ and ‘spread’), each with a distinctive morphology and K^+ conductance (Arkett et al., 1992). ‘Rounded’ osteoclasts are dome-shaped, lack lamellipodia and exhibit a transient, outwardly rectifying K^+ conductance. In contrast, ‘spread’ osteoclasts are flattened with lamellipodia, lack the outward K^+ conductance, but exhibit an inwardly rectifying K^+ conductance (Sims and Dixon, 1989; Sims et al., 1991; Arkett et al., 1992; Kelly et al., 1992). Although the physiological roles of these K^+ channels are unknown, they likely affect the activity of the electrogenic H^+-ATPase, which is directly responsible for acidification of the resorption lacunae, and hence bone resorption (Blair and Schlesinger, 1992).

Inwardly rectifying K^+ channels have been identified in a

number of different types of cells, including macrophages, cells closely related to osteoclasts (Gallin, 1991). Although this K^+ conductance in macrophages and some other cells is regulated by G proteins (Fargon et al., 1990; McCloskey and Cahalan, 1990; McKinney and Gallin, 1992), it is not known whether G proteins regulate this K^+ conductance in osteoclasts. The purpose of our study was to examine the role of G proteins in regulating osteoclast ionic conductances and morphology. Hydrolysis-resistant GTP analogues and fluoroaluminate were introduced directly into single osteoclasts using a patch-clamp electrode. Changes in cell morphology were monitored concurrently by video microscopy. Using this combined approach, we were able to quantify changes in morphology, capacitance and ionic currents of intact osteoclasts. We describe below the effects of guanosine 5′-*O*-(3-thiotriphosphate) and fluoroaluminate on osteoclast morphology and K^+ current, and show that motility and ion transport are regulated by separate G-protein-coupled pathways.

MATERIALS AND METHODS

Osteoclast isolation

Isolation of osteoclasts has been described previously (Arkett et al., 1992). Briefly, osteoclasts were isolated from *femora* and *tibiae* of Wistar rat pups and plated onto sterile glass coverslips. Non-adherent cells and debris were removed by washing coverslips with phosphate-buffered saline. Osteoclasts were incubated (5% CO_2; 37°C) in Medium 199 (Gibco), buffered with Hepes and HCO_3^-, and supplemented with heat-inactivated foetal bovine serum (15%) and antibiotics. Osteoclasts were studied within 12 hours of isolation.

Electrophysiological recording

Conventional whole-cell, patch-clamp techniques were used. Time of establishing whole-cell configuration ('break-in') served as an initial reference point for all experiments and was defined as time 0. The standard electrode solution consisted of (in mM): KCl, 140; Hepes, 20; $MgCl_2$, 1; $CaCl_2$, 0.4; EGTA, 1 (estimated free $[Ca^{2+}] \approx 100$ nM); pH 7.2 (adjusted with KOH); 280 to 290 mosmol/l. For high Ca^{2+} experiments, we adjusted free $[Ca^{2+}]$ in the electrode solution to 1 μM. In some cases, we modified the standard electrode solution to a reduced Cl^- concentration by using 20 mM KCl and 120 mM K aspartate. Hydrolysis-resistant GTP analogues, fluoroaluminate and other agents were introduced into cells by including these substances in the electrode solution. Unless stated otherwise, the concentration of nucleotides in the patch pipette was 250 μM. NaF (1 mM) and $AlCl_3$ (25 μM) were added to standard electrode solution to form fluoroaluminate complexes. Electrode capacitance was reduced by coating the electrode with beeswax. After polishing, electrode resistance was 5 to 8 MΩ. Currents were recorded with an Axopatch-1B amplifier (Axon Instruments, Foster City, CA) filtered (-3 dB at 1 kHz), and digitized at 2 to 5 kHz using pClamp Version 5.5 (Axon Instruments). Access resistance was usually <10 MΩ. We minimized series resistance error by routinely using 80% series resistance compensation. Whole-cell capacitance, which is a measure of the total surface area, was determined from capacitance compensation circuitry on the amplifier or by digital integration of capacitive transients. Cells were bathed in a standard saline consisting of (in mM): NaCl, 130; KCl, 5; Hepes, 20; glucose, 10; $MgCl_2$, 1; $CaCl_2$ 1; pH 7.4 (adjusted with NaOH); 280 to 290 mosmol/l. All experiments were conducted at room temperature, 22 to 25°C.

Osteoclast imaging and area measurement

We viewed cells using phase-contrast optics and recorded images on videotape with a video camera (Sony CCD AVC-D5) or on 35 mm film. Planar area of osteoclasts was measured from video recordings using a computerized video-image analysis system and JAVA software (Jandel Scientific, Corte Madera, CA). We measured planar area at two-minute intervals and expressed cell area as a percentage of initial (i.e. at break-in) planar area. Fractional changes in planar area were normalized using the arcsine transformation before statistical analysis.

Nucleotides and other agents

Guanosine 5′-*O*-(3-thiotriphosphate) (GTPγS) was purchased from Boehringer-Mannheim (Montreal, Quebec) and Calbiochem (La Jolla, CA). Guanosine 5′-*O*-(2-thiodiphosphate) (GDPβS) was obtained from Calbiochem. Adenosine 5′-*O*-(3-thiotriphosphate) (ATPγS); adenosine 5′-triphosphate (ATP); guanosine 5′-triphosphate (GTP); 5′-guanylyl-imidodiphosphate (GppNHp); 8-bromoadenosine 3′,5′-cyclic monophosphate (8-bromo cAMP); 4-acetamido-4′-isothiocyanostilbene-2,2′-disulphonic acid (SITS); β-nicotinamide adenine dinucleotide (NAD); cytochalasin D; and colchicine were from Sigma Chemical Co. (St Louis, MO). Islet-activating protein (pertussis toxin) and pertussis toxin A protomer were from List Biological Laboratories, Inc. (Campbell, CA).

RESULTS

Using phase-contrast microscopy, we identified osteoclasts on the basis of multinuclearity; that is, the presence of three or more nuclei, as described previously (Sims and Dixon, 1989; Sims et al., 1992; Kelly et al., 1992; Arkett et al., 1992). Upon introduction of hydrolysis-resistant GTP analogues into the cytoplasm of 'spread' osteoclasts, we observed: (1) an increase in planar area; and (2) suppression of the current carried through inwardly rectifying K^+ channels. In contrast, GTP analogues had little effect on morphology or currents in 'rounded' osteoclasts (15 cells). Therefore, we focused specifically on the effects of G protein activation in the 'spread' phenotype. We will consider the effects of hydrolysis-resistant GTP analogues first on osteoclast morphology and then on the inwardly rectifying K^+ conductance. Finally, we consider the effects of fluoroaluminate, a selective activator of large molecular mass, heterotrimeric G proteins (Kahn, 1991).

Hydrolysis-resistant GTP analogues induce spreading

Within 1 minute of break-in with GTPγS in the patch pipette, osteoclast lamellipodia began to extend. After several minutes, lamellipodia, which were initially distinct, began to fuse forming an extended cell periphery (Fig. 1A). The continuous extension of cell periphery, or spreading, occurred concomitantly with a decrease in cell height, resulting in a progressively more flattened cell. In some cases, where 'spread' osteoclasts initially exhibited retraction fibres, the increase in peripheral membrane followed the fibres and filled in spaces between fibres and lamellipodia (Figs 1A, 2A). Most osteoclasts also exhibited dynamic ruffling of the plasma membrane as they spread (see Fig. 3). Spreading was observed in all 25 cells tested with GTPγS in the patch pipette and all 5 cells tested with GppNHp, another hydrolysis-resistant GTP analogue (Fig. 1B).

We quantified the change in area of osteoclasts by measuring the planar area of cells from the video record before and during introduction of G protein activators and control agents. Planar area was determined by measuring the area

delimited by the periphery of the plasma membrane, excluding retraction fibers. For example, Fig. 2A shows the periphery of the osteoclast in Fig. 1A before (broken line) and 10 minutes after (continuous line) introduction of GTPγS. Cell periphery extends centrifugally in response to GTPγS and individual lamellipodia fuse, leading to a more uniform periphery. Fig. 2B shows a plot of the changes in planar area over time after introduction of test substances. Both GTPγS and GppNHp induced a marked, continuous increase in planar area, beginning within 1 minute after break-in. Correlation analysis on a subsample of osteoclasts tested showed a significant positive correlation between area and time after break-in with GTPγS or GppNHp in the pipette.

To determine the specificity of GTPγS- and GppNHp-induced spreading, we examined the effects of several other nucleotides on cell morphology. GDPβS, a hydrolysis-resistant guanine nucleotide that does not activate G proteins, did not induce spreading in any of the eight cells tested (Figs 1C, 2B). In a few cases, GDPβS caused a slight reduction in planar area (e.g. see Fig. 1C). We did not attempt to reduce GTPγS-induced spreading by simultaneously including an equimolar amount of GDPβS. ATPγS did not induce spreading in five cells tested (Figs 1D, 2B), suggesting that the GTPγS-induced effect on morphology is specific for guanine nucleotides. Neither GTP (500 μM) in the pipette (4 cells), nor GTPγS applied extracellularly (3 cells) caused spreading (not shown). Thus, spreading was caused, or induced, specifically by intracellular hydrolysis-resistant guanine nucleotides, suggesting the involvement of a G protein.

Pertussis toxin, which inactivates certain G proteins through ADP ribosylation of the α subunit (Ui, 1990), has been reported to block receptor-independent activation of G proteins by hydrolysis-resistant GTP analogues in some cells (McCloskey and Cahalan, 1990; McKinney and Gallin, 1992). We incubated osteoclasts with pertussis toxin (0.5 to 5 μg/ml, holomer) for up to 6 hours. In all seven cells tested under these conditions, GTPγS still induced spreading (Fig. 3A,C). Since pertussis toxin did not alter the response to GTPγS, we considered the possibility that osteoclasts lack binding sites for pertussis toxin, and therefore cannot internalize the A protomer (Ui, 1990). To avoid this possible limitation, we included in the pipette, in addition to GTPγS (250 μM), the activated A protomer (S1 subunit; 200 ng/ml), together with necessary substrates, NAD (10 μM) and ATP (0.5 mM). In all five cells tested with A protomer, osteoclasts spread (Fig. 3B,C) in a manner similar to that seen without pertussis toxin (cf. Figs 1A,B, 2B).

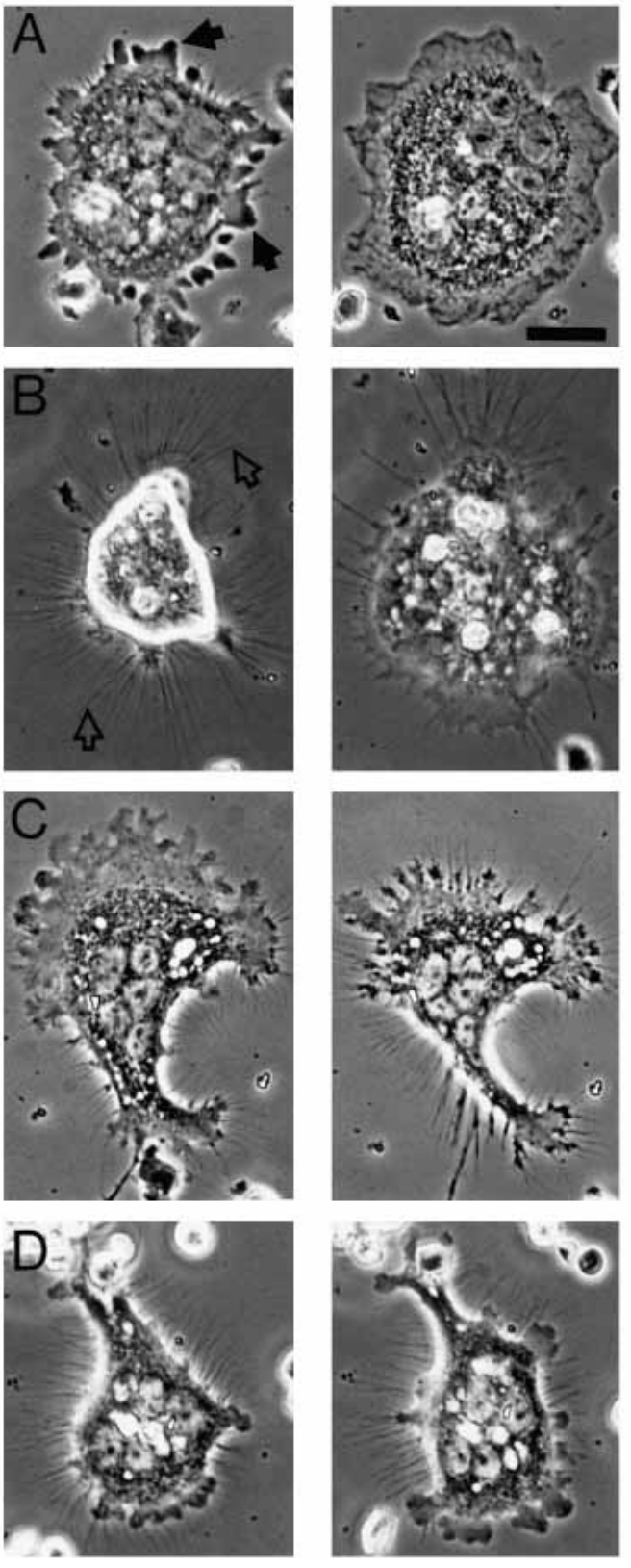

Fig. 1. Hydrolysis-resistant GTP analogues induce spreading in osteoclasts. (A) Osteoclast with distinct lamellipodia (arrows) ~1 minute before (left) introduction of GTPγS. Same osteoclast 10 minutes after introduction of GTPγS (250 μM) in standard electrode solution and removal of patch pipette (right). Note that membrane has extended in all directions, leading to fusion of lamellipodia. Bar, 20 μm (A, B, C, D). (B) Another osteoclast just before (left) introduction of GppNHp. Note that retraction fibers are prominent (arrows) and the cell is plump as indicated by the phase-bright edges. Same cell, 34 minutes after break-in (right) with GppNHp (250 μM) in pipette, has flattened and spread. (C) Osteoclast before (left) introduction of control agent GDPβS. Same cell, ~12 minutes after break-in (right) with GDPβS (250 μM) in pipette, has not spread but in this case retracted slightly. (D) Another osteoclast, just before (left) and ~19 minutes after (right) introduction of another control agent ATPγS (250 μM), does not show the spreading as in (A) or (B).

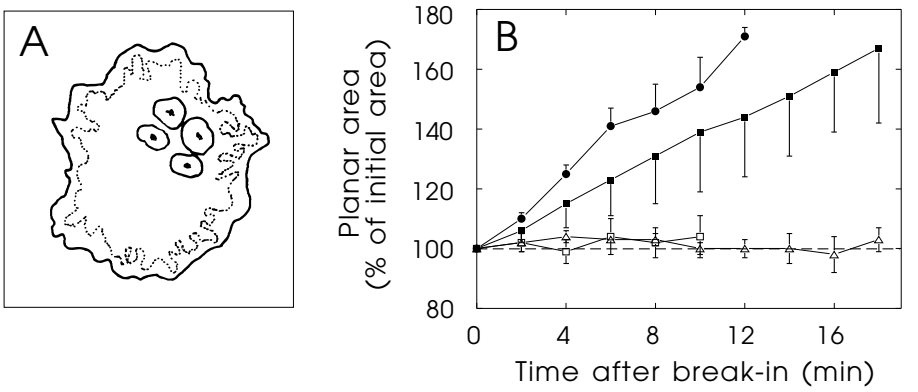

Fig. 2. Quantification of changes in planar area of osteoclasts. (A) To illustrate the method for quantification of cell planar area, tracings of osteoclast in Fig. 1A are shown prior to break-in (broken line) and 10 minutes after introduction of GTPγS (continuous line). Retraction fibres were excluded from cell measurements. This osteoclast showed an increase in planar area of 48%. (B) Plot of osteoclast planar area against time after break-in with GTPγS (●), GppNHp (■), ATPγS (△) or GDPβS (□), all at 250 μM. Data are mean ± s.e.m. planar area expressed as a percentage of initial area at time 0. GTPγS or GppNHp induced a significant increase in area with increased time after break-in, while GDPβS or ATPγS did not induce a significant change in planar area. Correlation analysis showed a significant positive correlation between area and time after break-in for GTPγS (r=0.82; P<0.001; n=41, 8 cells) or GppNHp (r=0.46; P<0.05; n=46; 5 cells), but no significant correlation for GDPβS (r=0.13; P>0.05; n=17; 3 cells) or ATPγS (r=0.03; P>0.05; n=18; 3 cells). In all cases, n is the total number of area measurements from cells within each test group.

Cytochalasin D, but not colchicine, inhibits GTPγS-induced spreading

To investigate the role of the cytoskeleton in GTPγS-induced spreading, we first examined the effects of cytochalasin D, which binds to actin with high affinity and disrupts its polymerization (Cooper, 1987). Cytochalasin D (5 μM) added to the bathing medium caused prompt retraction of lamellipodia, leaving retraction fibers (Fig. 4A,B). Planar area steadily decreased to 65±5% (mean ± s.e.m., 3 cells) of the initial planar area by 8 minutes, after which little change occurred. Subsequent introduction of GTPγS did not induce spreading (Fig. 4B,D). On the other hand, colchicine (10 to 100 μM), which prevents polymerization of tubulin, caused only slight retraction of osteoclasts. Moreover, subsequent introduction of GTPγS to colchicine-treated osteoclasts still induced spreading (Fig. 4C,D), to an extent comparable to that seen with GTPγS alone (cf. Figs 1A, 2B). These findings indicate that GTPγS-induced spreading is dependent upon actin polymerization.

GTPγS-induced suppression of the inwardly rectifying K^+ current

When studied under voltage clamp, 'spread' osteoclasts show an inward current in response to hyperpolarizing voltage commands, and little outward current in response to depolarizing commands. This inwardly rectifying K^+ current has been characterized (Sims and Dixon, 1989; Sims et al., 1991; Arkett et al., 1992). To examine the effects of GTPγS on this K^+ current, we included GTPγS in the electrode solution. Under these conditions, 'spread' osteoclasts exhibited the typical inwardly rectifying K^+ current immediately after break-in (Fig. 5A). We monitored the K^+ current over time with periodic voltage steps to −100 mV. Inwardly rectifying K^+ current was steady for 5 to 8 minutes, after which it declined in amplitude until barely detectable (Fig. 5). In contrast, this K^+ current persisted under control conditions (Figs 6, 7B). Suppression of K^+ current similar to that illustrated in Fig. 5 was observed in 20 out of 22 osteoclasts when GTPγS was included in the pipette. Like GTPγS, GppNHp also suppressed the K^+ current (Fig. 7A; 4 cells). Additionally, GTPγS-induced suppression of the K^+ current was unaltered in the presence of colchicine (3 cells) or cytochalasin D (4 cells) (Fig. 7A).

Following suppression of the K^+ current, there remained residual current consisting of a Cl^- current known to be exhibited by these osteoclasts (Sims et al., 1991) and a linear leak current. In Fig. 5, we used a low Cl^- electrode solution to minimize the Cl^- current at the voltages where we measured K^+ current, thereby more clearly revealing the time course of K^+ current decline. However, in most experiments, we used the standard electrode solution with a calculated equilibrium potential for Cl^- of 0 mV. In these experiments, the residual current following GTPγS-induced suppression of the K^+ current consisted of a noninactivating current that reversed direction at 0 mV and was blocked by 1 mM SITS (not shown). This residual current resembled the Cl^- current described previously in osteoclasts (Sims et al., 1991; Kelly et al., 1994). The Cl^- current did not appear to be regulated by hydrolysis-resistant GTP analogues.

As controls for the effects of GTPγS on the K^+ current, we examined the effects of several other nucleotides. The inwardly rectifying K^+ current did not decline when GTP (500 μM) was included in the patch pipette. Fig. 6 illustrates this finding by showing that the K^+ current, elicited at −100 mV, remained largely unchanged 10 minutes after break-in with GTP in the pipette. Similar results were observed in all four cells tested. To demonstrate that the inward K^+ current was indeed still present, we briefly applied Ba^{2+} (1 mM), which rapidly and reversibly blocked the inwardly rectifying K^+ current (Fig. 6 A,B), as previously described (Sims and Dixon, 1989). Similar persistence of the K^+ current was also observed when ATPγS (4 cells) or GDPβS (7 cells) was included or when no nucleotides were included in the standard pipette solution (16 cells) (Fig. 7B). Thus, hydrolysis-resistant GTP analogues induce suppression

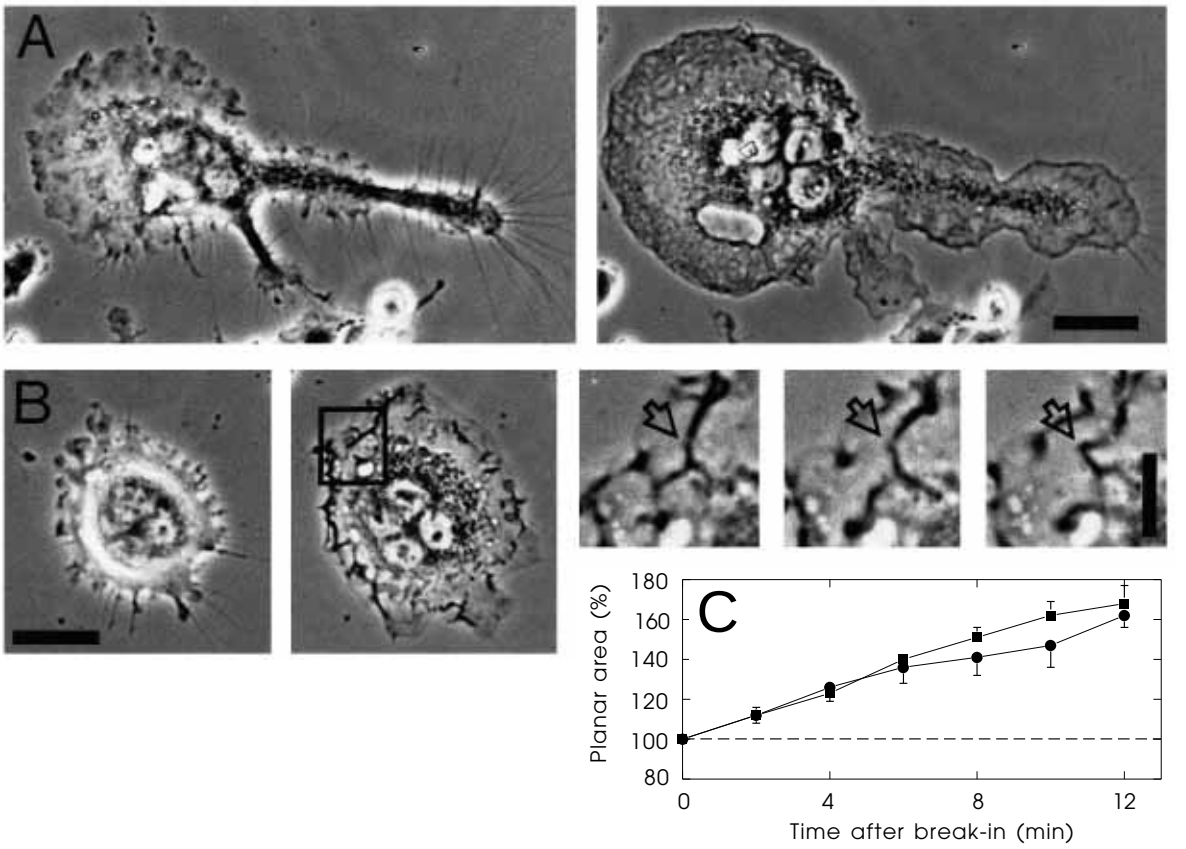

Fig. 3. GTPγS-induced spreading is not affected by pertussis toxin. (A) At left is an osteoclast 6 hours after addition of pertussis toxin (0.5 μg/ml) and just prior to introduction of GTPγS (250 μM) via patch pipette. Panel at right shows the same osteoclast 11 minutes after break-in. Planar area increased markedly, indicating that pertussis toxin did not block GTPγS-induced spreading. Bar, 20 μm. (B) At left is an untreated osteoclast just prior to break-in. At right is the same osteoclast 9 minutes after break-in with a patch pipette containing the A protomer of pertussis toxin (200 ng/ml), NAD (10 μM), ATP (0.5 mM), and GTPγS (250 μM). Planar area increased markedly, indicating that the A protomer of pertussis toxin did not block GTPγS-induced spreading. Bar, 20 μm. The three panels at the far right show a portion of the osteoclast (indicated by box) at ~1 minute intervals starting 11 minutes after break-in. Bar, 10 μm. Changes in the pattern of the phase-dark structures (arrows) indicate dynamic ruffling of the plasma membrane. (C) Plot of osteoclast planar area against time after break-in with GTPγS (250 μM) after pre-treatment with pertussis toxin (●) or inclusion of A protomer of pertussis toxin in pipette (■). Data are means ± s.e.m. planar area expressed as a percentage of initial area. Correlation analysis showed a significant positive correlation between area and time after break-in after pertussis toxin pre-treatment (r=0.84; P<0.001; n=20; 3 cells) and after inclusion of A protomer in pipette (r=0.90; P<0.001; n=35; 5 cells).

of the inwardly rectifying K^+ current in osteoclasts, since this effect was observed specifically upon introduction of GTPγS and GppNHp, but not GTP, GDPβS or ATPγS.

GTPγS-induced suppression of K^+ current is unaffected by pertussis toxin and not mimicked by second messengers

We investigated the effects of pertussis toxin on the G protein that may be involved in regulating the K^+ current, using the holotoxin and the A protomer as described above. Osteoclasts were pre-treated with the holotoxin (5 μg/ml) for up to 6 hours. In all seven cells tested, GTPγS induced a suppression of the inwardly rectifying K^+ current in a manner similar to that observed in untreated cells (Fig. 7A). Inclusion of the activated A protomer, NAD, ATP, along with GTPγS in six cells induced a similar suppression of the K^+ current (not shown). Thus, it appears that GTPγS-induced suppression of the inwardly rectifying K^+ current is insensitive to pertussis toxin.

To investigate possible mechanisms underlying G protein-induced suppression of the inwardly rectifying K^+ current, we altered the cellular concentrations of selected second messengers. Instead of including hydrolysis-resistant GTP analogues in the pipette, we elevated intracellular Ca^{2+} by using electrode solution with a calculated free [Ca^{2+}] of 1 μM or by extracellular application of the Ca^{2+} ionophore, A23187 (1 μM). Neither of these treatments had any effect on the K^+ current in 15 cells (Fig. 7B). Likewise, 8-bromo cAMP applied extracellularly (1 mM) or included in the patch pipette (0.5 mM) had no effect on the K^+ current in 8 cells (Fig. 7B).

GTPγS does not induce changes in whole-cell capacitance

In some cell types, hydrolysis-resistant GTP analogues induce exocytosis and an increase in cell surface area, which can be detected as an increase in whole-cell capacitance (Oberhauser et al., 1992). Using the capacitance compensation circuitry on

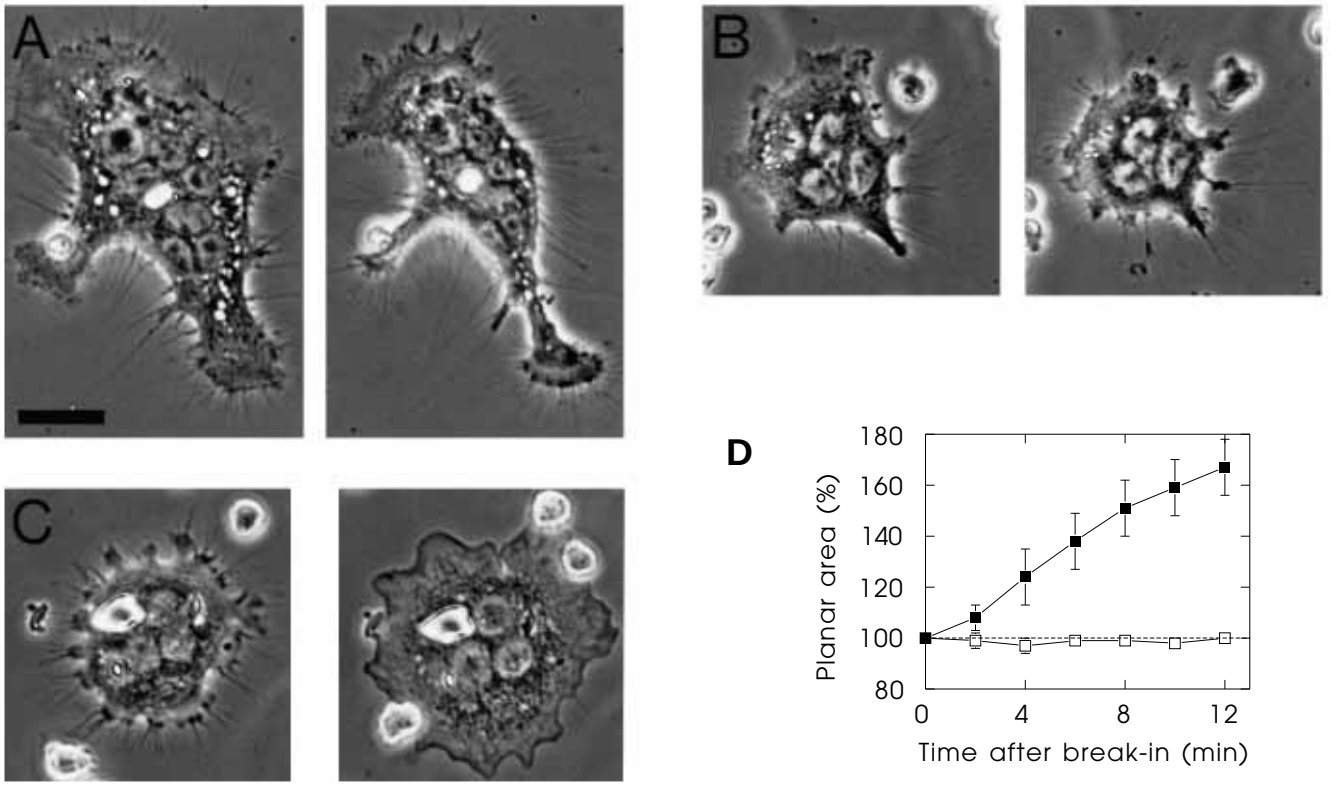

Fig. 4. GTPγS-induced spreading is inhibited by cytochalasin D but not by colchicine. (A) Osteoclast just before (left) and 11 minutes after (right) addition of 5 μM cytochalasin D to the bath. Planar area of osteoclast decreased. (B) At left is another osteoclast 6 minutes after addition of cytochalasin D (5 μM) and just before break-in. At right is the same osteoclast 8 minutes after break-in with GTPγS (250 μM) in the pipette. Planar area did not increase, indicating that cytochalasin D blocked GTPγS-induced spreading. (C) Panel at left shows an osteoclast 12 minutes after addition of colchicine (10 μM) and just prior to break-in. At right is the same osteoclast 14 minutes after break-in with GTPγS (250 μM) in the patch pipette. Planar area increased markedly, indicating that colchicine did not block GTPγS-induced spreading. (D) Plot of osteoclast planar area against time after break-in with GTPγS (250 μM) in the pipette following pre-treatment with either 5 μM cytochalasin D (□; 3 cells) or 10 μM colchicine (■; 3 cells). Data are means ± s. e. m. of planar area expressed as a percentage of initial area. Correlation analysis showed no significant correlation between area and time after break-in after pre-treatment with cytochalasin D (r=0.04; P>0.05; n=21; 3 cells), but significant positive correlation after pre-treatment with colchicine (r=0.86; P<0.001; n=21; 3 cells). Bar, 20 μm (A,B,C).

the amplifier or digital integration of capacitive transients, we monitored whole-cell capacitance throughout the course of recordings. None of the osteoclasts tested with GTPγS showed notable changes in whole-cell capacitance during GTPγS-induced suppression of K^+ current. For example, the cell in Fig. 5 had an initial whole-cell capacitance of 37 pF and the same capacitance after the K^+ current was suppressed. Since GTPγS did not alter whole-cell capacitance, we conclude that total membrane area did not change appreciably during spreading or K^+ current suppression.

Spreading and K^+ current suppression are regulated by different G proteins

As shown above, inclusion of hydrolysis-resistant GTP analogues in the patch pipette induced spreading within 2 minutes of break-in, yet suppression of the inwardly rectifying K^+ current typically began after a delay of 5 to 8 minutes. Fig. 8A illustrates the difference in time course for these two events in the same cell. In every osteoclast where we were able to maintain high resistance recordings long enough to observe suppression of the K^+ current, an increase in area was also observed (43 cells). Since GTPγS-induced spreading preceded changes in K^+ current, it seems unlikely that the lag in onset of K^+ current suppression results from delayed diffusion of GTPγS. Alternatively, we considered the possibility that different G proteins mediate these events.

Fluoroaluminate has been demonstrated to be a useful tool in differentiating the involvement of monomeric and heterotrimeric G proteins in signalling pathways (Kahn, 1991). In all five osteoclasts tested, inclusion of NaF (1 mM) and $AlCl_3$ (25 μM) in the pipette failed to induce spreading (Fig. 8B). Ten minutes after break-in with fluoroaluminate in the pipette, the planar area was 91% (± 1.1; 5 cells) (mean ± s. e. m.) of initial area, compared to 154% (±9.8; 4 cells) 10 minutes after break-in with GTPγS (cf. Fig. 2B). However, fluoroaluminate did suppress the K^+ current to an extent and after a delay comparable to that observed with GTP analogues (Fig. 8B). The differential effects of hydrolysis-resistant nucleotide analogues and fluoroaluminate on cell spreading and K^+ current suggest that different G proteins are involved in regulating osteoclast spreading and inwardly rectifying K^+ current.

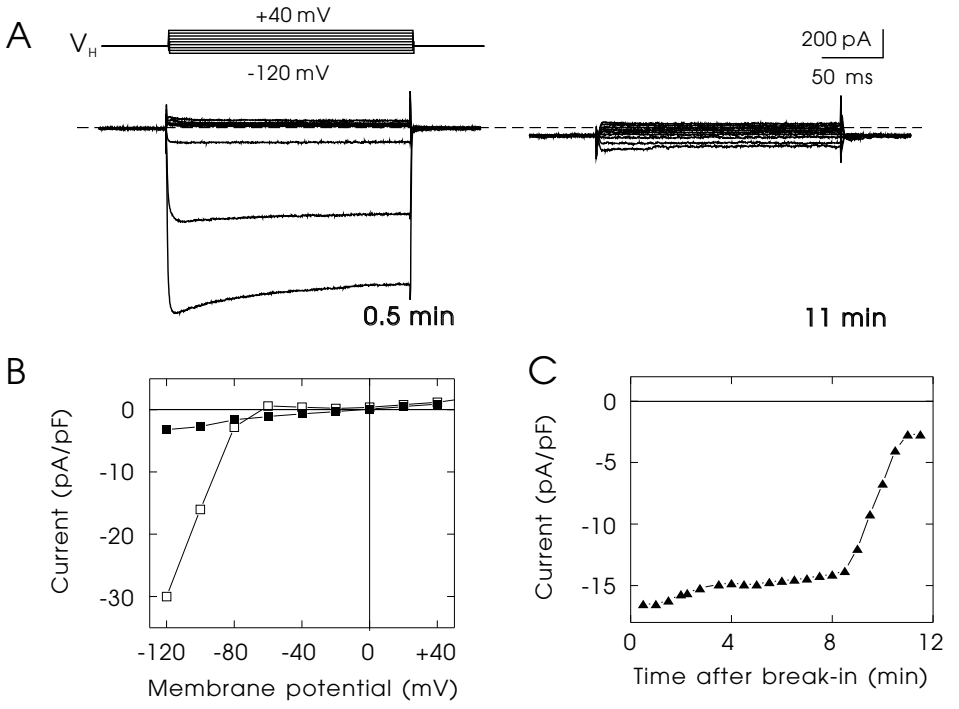

Fig. 5. GTPγS-induced suppression of the inwardly rectifying K^+ current. (A) Currents elicited in a 'spread' osteoclast by a series of voltage commands (shown above) given at 1 Hz from a holding potential (V_H) of −70 mV. Currents recorded 0.5 minute after break-in (left) were dominated by an inwardly rectifying K^+ current. Patch pipette contained the low Cl^- electrode solution and 250 μM GTPγS. At right are residual currents, recorded from the same osteoclast 11.5 minutes after break-in. K^+ current is nearly completely suppressed. Broken line represents zero current level. (B) Current/voltage plot from average current values in A (between 150 and 190 ms after onset of voltage commands) 0.5 minute (□) and 11.5 minutes (■) after break-in. Inwardly rectifying K^+ current, which was present initially, was absent after 11.5 minutes. Current/voltage plot shows the residual current as a near linear 'leak' conductance. (C) Plot of current at −100 mV recorded at various times after break-in. Magnitude of K^+ current changed negligibly up to ~8 minutes, after which K^+ current declined rapidly. Whole-cell capacitance (37 pF) did not change over the course of the recording.

DISCUSSION

Activation of G proteins induces osteoclast spreading

We have shown that upon introduction of hydrolysis-resistant GTP analogues (GTPγS or GppNHp) into the cytoplasm, lamellipodia of 'spread' osteoclasts extend and spread centrifugally. This effect, which occurred concomitantly with reduction in cell height, resulted in a significant increase in osteoclast planar area. This increase in planar area arose from rearrangement of existing plasma membrane rather than addition of new membrane, by exocytosis. This conclusion is based on our finding that whole-cell capacitance, which is a measure of total surface area, did not change over the course of GTPγS-induced spreading. If the increase in planar area had occurred by exocytosis, we would have expected increases in cell capacitance of ~50% by 8 minutes (e.g. Fig. 8A), a change that we could easily have detected using whole-cell recording.

In contrast to the effect of GTPγS and GppNHp, inclusion of GDPβS in the pipette did not cause spreading. GDPβS is a hydrolysis-resistant GDP analogue that competes with GTP for binding sites on G proteins but, unlike GTPγS, does not activate them. Since addition of GDPβS did cause a slight retraction of some cells, it is conceivable that GDPβS inhibited endogenous G protein activity. Extracellular application of GTPγS did not induce spreading, ruling out the possibility that these effects arise from activation of cell surface nucleotide receptors. Additionally, ATPγS did not induce spreading, indicating specificity for hydrolysis-resistant guanine nucleotides. Taken together, these findings are consistent with a role for G proteins in the regulation of osteoclast spreading.

G-protein-induced osteoclast spreading is dependent upon actin polymerization

We have shown that lamellipod extension induced by activation of G proteins is blocked by cytochalasin D, but not by colchicine. Cytochalasin D is known to block specifically actin polymerization (Cooper, 1987; Ohmori et al., 1992), suggesting its involvement in GTPγS-induced spreading of osteoclasts. Consistent with this suggestion, lamellipod extension is thought to involve conversion of globular (G) to filamentous (F) actin at the leading edge of lamellipodia or pseudopodia (Smith, 1988; Cassimeris et al., 1990; Cooper, 1991). In osteoclasts, F-actin has been shown, by staining with labelled phalloidin, to be concentrated at the edges of lamellipodia (Turksen et al., 1988; Lakkakorpi and Väänänen, 1991).

Hydrolysis-resistant guanine nucleotides have been shown to increase F-actin content in neutrophils. Upon their electropermeabilization, F-actin content promptly increases in the presence of GTPγS, reaching a steady level of 250% of initial content after 5 to 10 minutes (Bengtsson et al., 1990). Using the same technique to introduce GTPγS, Therrien and Naccache (1989) found an increase of ~75% in initial F-actin content by 1 minute, while Downey and co-workers (1989) reported a maximum F-actin content within 2 minutes. We detected a marked increase in the planar area of osteoclasts within 1 to 2 minutes of introduction of GTPγS, with cells spreading to 150% of initial area by ~8 minutes. In none of the above mentioned studies did pre-treatment with pertussis toxin alter the increase in F-actin content induced by activation of G proteins. Likewise, GTPγS-induced spreading of osteoclasts was insensitive to pertussis toxin. Thus, similarities in regulation of actin polymerization in neutrophils and spreading in osteoclasts support our contention that actin polymerization underlies G protein-mediated spreading.

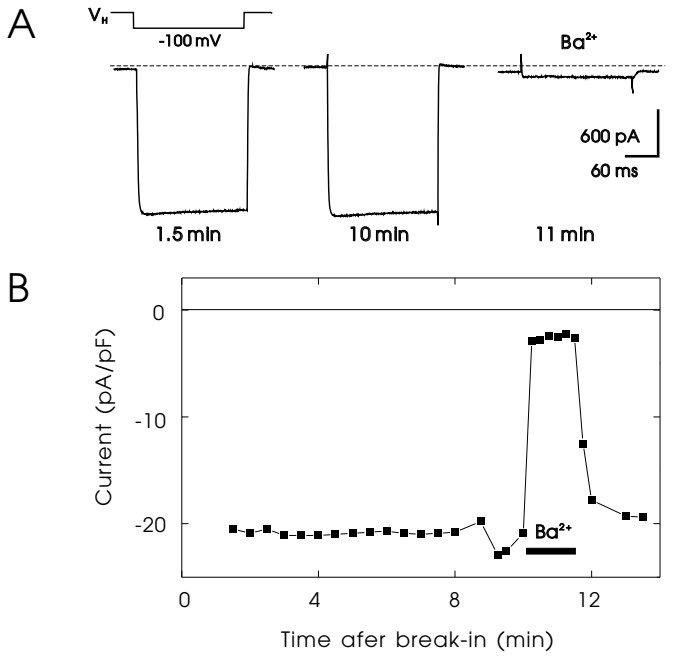

Fig. 6. Inwardly rectifying K^+ current persists in presence of GTP. (A) Currents elicited in an osteoclast at −100 mV (shown above) from a holding potential (V_H) of −70 mV at various times after break-in with GTP (500 μM) in patch pipette with standard electrode solution. The inwardly rectifying K^+ current recorded at −100 mV is unchanged 10 minutes after break-in. External Ba^{2+} (1 mM), applied extracelluarly just before trace at far right was recorded, reversibly blocked this K^+ current. Broken line indicates zero current level. Cell capacitance (89 pF) did not change over the course of the recording. (B) Plot of the K^+ current at −100 mV recorded from cell in (A) at various times after break-in. K^+ current amplitude was steady throughout recording, and was reversibly blocked by 1 mM Ba^{2+} (filled bar).

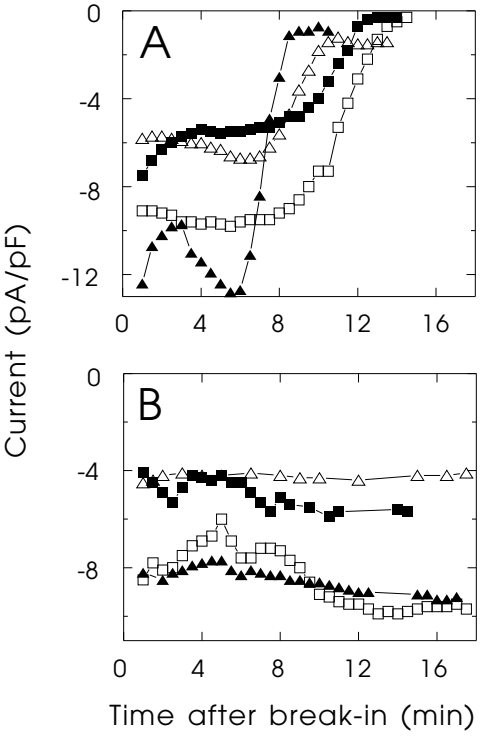

Fig. 7. Inhibition of K^+ current by hydrolysis-resistant GTP analogues and persistence under control conditions. (A) Plot of current at −100 mV recorded at various times after break-in with GppNHp (■) in pipette, GTPγS in pipette after a 4.5 hour pre-treatment with pertussis toxin (△, 1 μg/ml), GTPγS in pipette after pre-treatment with colchicine (□, 10 μM), or cytochalasin D (▲, 5 μM). Concentration of GTPγS or GppNHp was 250 μM in standard electrode solution. GTPγS-induced suppression of K^+ current was not altered by pertussis toxin, colchicine or cytochalasin D. (B) Plot of current at −100 mV recorded at various times after break-in with ATPγS (□, 250 μM), GDPβS (■, 250 μM), 8-bromo cAMP (▲, 500 μM) included in standard electrode solution or high (1 μM) Ca^{2+} electrode solution (△). Inwardly rectifying K^+ current persisted with control solutions (ATPγS, GDPβS) and was unaltered by increased intracellular [Ca^{2+}] or [cAMP].

We have shown that two second messengers (Ca^{2+}, cyclic AMP), which may be generated following activation of G-protein-coupled enzymes, did not induce spreading in rat osteoclasts. In neutrophils and lymphocytes, actin polymerization is induced by membrane-permeant diacylglycerols and blocked by protein kinase inhibitors (Zimmermann et al., 1988; Keller et al., 1989; Apgar, 1991), suggesting the involvement of protein kinase C. However, others have shown that osteoclast spreading is not induced by phorbol myristate acetate, an activator of protein kinase C (Murrills et al., 1992; Teti et al., 1992). It has been proposed that osteoclast retraction and inhibition of motility are mediated by separate G-protein-coupled signalling pathways (Zaidi et al., 1990). However, these morphological responses are clearly different from those reported in the present study.

Activation of G protein suppresses inwardly rectifying K^+ current

We have shown that GTPγS, GppNHp, as well as fluoroaluminate, suppress the inwardly rectifying K^+ current in rat osteoclasts, indicating the involvement of a G protein. Following a delay of 5 to 8 minutes, the K^+ current declined rapidly and became undetectable within 7 to 10 minutes. Such GTPγS-induced suppression of inwardly rectifying K^+ current has been shown in other cell types. The inwardly rectifying K^+ current exhibited by a mast cell line gradually declines in amplitude over prolonged whole-cell recordings, when no nucleotides have been added to the pipette (McCloskey and Cahalan, 1990). Inclusion of GTPγS, GppNHp or fluoroaluminate in the pipette induced, after a variable delay, more rapid decline of the mast cell K^+ current with a half-time for decay of ~5 minutes. A similar GTPγS-induced decline in the amplitude of the inwardly rectifying K^+ current has been shown in enterocytes (Fargon et al., 1990), as well as macrophages (McKinney and Gallin, 1992). As reported for both mast cells and macrophages (McCloskey and Cahalan, 1990; McKinney and Gallin, 1992) and shown here for osteoclasts, GTPγS-induced suppression of the inwardly rectifying K^+ current was not affected by pertussis toxin. However, these findings do not eliminate the possibility that receptor-mediated activation of this G protein is sensitive to pertussis toxin. Notably, in both mast cells and macrophages, GTPγS also

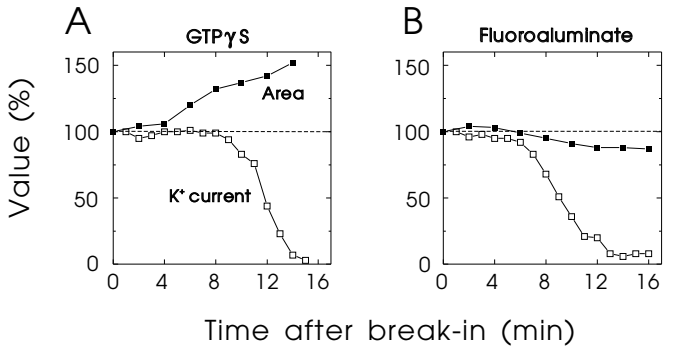

Fig. 8. Differential effects of GTPγS and fluoroaluminate on area and K^+ current. (A) Plot of concomitant changes in planar area (■) and K^+ current at −100 mV (□) in the same cell at various times after break-in with GTPγS (250 μM) in the patch pipette containing standard electrode solution. Data are planar area expressed as a percentage of initial area or K^+ current expressed as a percentage of initial K^+ current. The increase in planar area began shortly after break-in. However, K^+ current amplitude remained unchanged up to ~8 minutes after break-in, after which time the K^+ current declined. Cell capacitance (91 pF) remained unchanged throughout the recording. (B) Plot of planar area (■) and K^+ current at −100 mV (□) in another cell at various times after break-in with NaF (1 mM) and $AlCl_3$ (25 μM) in the patch pipette containing standard electrode solution. Data are planar area expressed as a percentage of initial area or K^+ current expressed as a percentage of initial K^+ current. Planar area changed only slightly throughout recording, even though the K^+ current declined after a delay of ~5 minutes. Cell capacitance (30 pF) remained unchanged throughout the recording.

induced an outwardly rectifying K^+ conductance, an effect that was blocked by pertussis toxin (McCloskey and Cahalan, 1990; McKinney and Gallin, 1992). We did not observe a GTPγS-induced outwardly rectifying K^+ current in osteoclasts.

The delay of 5 to 8 minutes before the onset of GTPγS-induced K^+ current suppression in osteoclasts suggests an indirect effect of a G protein on the K^+ channel. Although slow diffusion of GTPγS could delay the decline in K^+ current, this explanation seems unlikely, since GTPγS-induced spreading began within 2 minutes after break-in, indicating that GTPγS had diffused rapidly throughout the cell. Alternatively, regulation of the inwardly rectifying K^+ current may involve G-protein-coupled enzymes and generation of second messengers. In this regard, we found no effects of elevation of cytosolic Ca^{2+} or a cAMP analogue on the inwardly rectifying K^+ current. Similarly, in other cell types, inwardly rectifying K^+ current is not suppressed by cAMP (Nakajima et al., 1988; Kurtz and Penner, 1989; McCloskey and Cahalan, 1990), inositol-1,4,5-trisphosphate (Kurtz and Penner, 1989; McCloskey and Cahalan, 1990), or activation of protein kinase C (Fargon et al., 1990).

Inhibition of osteoclast activity by calcitonin involves the selective internalization of the apical plasma membrane ('ruffled border') (Baron et al., 1990). It is possible that G protein-mediated regulation of the inwardly rectifying K^+ current results from redistribution of plasma membrane containing the K^+ channels. However, endocytosis of plasma membrane seems unlikely, since whole-cell capacitance of osteoclasts remained unchanged during GTPγS-induced suppression of the K^+ current. In addition, suppression of the K^+ current was not dependent upon spreading, or possible stretching of the membrane, since GTPγS reduced K^+ current even in the presence of cytochalasin D, which blocked cell spreading.

Osteoclast spreading and inwardly rectifying K^+ current are regulated by different types of G proteins

Whereas GTPγS activates both large heterotrimeric and small monomeric G proteins, fluoroaluminate activates only the heterotrimeric type of GTP-binding protein (Kahn, 1991). We have shown that hydrolysis-resistant GTP analogues induce both spreading and suppression of the inwardly rectifying K^+ current in osteoclasts. In contrast, although fluoroaluminate suppressed the K^+ current, it did not induce spreading. These findings suggest that the inwardly rectifying K^+ conductance is regulated by a heterotrimeric G protein, whereas actin-based lamellipodial spreading is regulated by a small molecular mass G protein. Thus, regulation of osteoclast motility and ion transport are regulated by different G protein-coupled pathways.

Small monomeric G proteins related to ras have been shown to be involved in regulating actin cytoskeleton in other cell types. Microinjection of rac into fibroblasts immediately induces F-actin accumulation in plasma membrane ruffles (Ridley et al., 1992), whereas rho induces the formation of stress fibers and focal adhesions (Ridley and Hall, 1992). Osteoclasts adhere to the extracellular matrix by F-actin-containing podosomes (Turksen et al., 1988; Lakkakorpi and Väänänen, 1991). Furthermore, osteoclast movement involves ruffling, as well as lamellipod extension and retraction. Our observation that small monomeric G proteins regulate lamellipod extension suggests an important role for these proteins in control of osteoclast motility, adhesion and chemotaxis, all of which are necessary for bone remodelling. In summary, osteoclast spreading and inwardly rectifying K^+ current are regulated by different types of G proteins. In this study, GTPγS activated both types of G proteins. However, under physiological conditions, these signalling pathways are likely to be regulated independently. The factors responsible for the physiological activation of these G proteins are yet to be determined.

We thank Dr Chris Ellis (Department of Medical Biophysics, The University of Western Ontario) for assistance with video-image analysis. This work was supported by The Arthritis Society and Medical Research Council of Canada. S. M. Sims is supported by a Scientist Award and S. J. Dixon by a Development Grant from the Medical Research Council of Canada.

REFERENCES

Apgar, J. R. (1991). Regulation of the antigen-induced F-actin response in rat basophilic leukemia cells by protein kinase C. *J. Cell Sci.* **112**, 1157-1163.

Arkett, S. A., Dixon, S. J. and Sims, S. M. (1992). Substrate influences rat osteoclast morphology and expression of potassium conductances. *J. Physiol.* **458**, 633-653.

Baron, R., Neff, L., Brown, W., Louvard, D. and Courtoy, P. J. (1990). Selective internalization of the apical plasma membrane and rapid redistribution of lysosomal enzymes and mannose 6-phosphate receptors during osteoclast inactivation by calcitonin. *J. Cell Sci.* **97**, 439-447.

Bengtsson, T., Särndahl, E., Stendahl, O. and Andersson, T. (1990). Involvement of GTP-binding proteins in actin polymerization in human neutrophils. *Proc. Nat. Acad. Sci. USA* **87**, 2921-2925.

Blair, H. C. and Schlesinger, P. H. (1992). The mechanism of osteoclast acidification. In *Biology and Physiology of the Osteoclast* (ed. B. R. Rifkin and C. V. Gay), pp. 259-287. CRC Press, Boca Raton, FL.

Cassimeris, L., McNeill, H. and Zigmond, S. H. (1990). Chemoattractant-stimulated polymorphonuclear leukocytes contain two populations of actin filaments that differ in their spatial distributions and relative stabilities. *J. Cell Biol.* **110**, 1067-1075.

Chabre, O., Conklin, B. R., Lin, H. Y., Lodish, H. F., Wilson, E., Ives, H. E., Catanzariti, L., Hemmings, B. A. and Bourne, H. R. (1992). A recombinant calcitonin receptor independently stimulates 3′, 5′-cyclic adenosine monophosphate and Ca^{2+}/inositol phosphate signalling pathways. *Mol. Endocrinol.* **6**, 551-556.

Cooper, J. A. (1987). Effects of cytochalasin and phalloidin on actin. *J. Cell Biol.* **105**, 1473-1478.

Cooper, J. A. (1991). The role of actin polymerization in cell motility. *Annu. Rev. Physiol.* **53**, 585-605.

Downey, G. P., Chan, C. K. and Grinstein, S. (1989). Actin assembly in electropermeabilized neutrophils: role of G-proteins. *Biochem. Biophys. Res. Commun.* **164**, 700-705.

Fargon, F., McNaughton, P. A. and Sepúlveda, F. V. (1990). Possible involvement of GTP-binding proteins in the deactivation of an inwardly rectifying K^+ current in enterocytes isolated from guinea-pig small intestine. *Pflügers Arch.* **417**, 240-242.

Gallin, E. K. (1991). Ion channels in leukocytes. *Physiol. Rev.* **71**, 775-811.

Hall, A. (1992). Ras-related GTPases and the cytoskeleton. *Mol. Biol. Cell* **3**, 475-479.

Kahn, R. A. (1991). Fluoride is not an activator of the smaller (20-25 kDa) GTP-binding proteins. *J. Biol. Chem.* **266**, 15595-15597.

Kanehisa, J. and Heersche, J. N. M. (1988). Osteoclastic bone resorption: In vitro analysis of the rate of resorption and migration of individual osteoclasts. *Bone* **9**, 73-79.

Keller, H. U., Niggli, V. and Zimmermann, A. (1989). Diacylglycerols and PMA induce actin polymerization and distinct shape changes in lymphocytes: relation to fluid pinocytosis and locomotion. *J. Cell Sci.* **93**, 457-465.

Kelly, M. E. M., Dixon, S. J. and Sims, S. M. (1992). Inwardly rectifying potassium current in rabbit osteoclasts: a whole-cell and single-channel study. *J. Membr. Biol.* **126**, 171-181.

Kelly, M. E. M., Dixon, S. J. and Sims, S. M. (1994). Outwardly rectifying chloride current in rabbit osteoclasts is activated by hypoosmotic stimulation. *J. Physiol.* (in press).

Kurtz, A. and Penner, R. (1989). Angiotensin II induces oscillations of intracellular calcium and blocks anomalous inward rectifying potassium current in mouse renal juxtaglomerular cells. *Proc. Nat. Acad. Sci. USA* **86**, 3423-3427.

Lakkakorpi, P. T. and Väänänen, H. K. (1991). Kinetics of the osteoclast cytoskeleton during the resorption cycle in vitro. *J. Bone Miner. Res.* **6**, 817-826.

McCloskey, M. A. and Cahalan, M. D. (1990). G protein control of potassium channel activity in a mast cell line. *J. Gen. Physiol.* **95**, 205-227.

McKinney, L. C. and Gallin, E. K. (1992). G-protein activators induce a potassium conductance in murine macrophages. *J. Membr. Biol.* **130**, 265-276.

Murrills, R. J. and Dempster, D. W. (1990). The effects of stimulators of intracellular cyclic AMP on rat and chick osteoclasts in vitro: Validation of a simplified light microscopic assay of bone resorption. *Bone* **11**, 333-344.

Murrills, R. J., Stein, L. S., Horbert, W. R. and Dempster, D. W. (1992). Effects of phorbol myristate acetate on rat and chick osteoclasts. *J. Bone Miner. Res.* **7**, 415-423.

Nakajima, Y., Nakajima, S. and Inoue, M. (1988). Pertussis toxin-insensitive G protein mediates substance P-induced inhibition of potassium channels in brain neurons. *Proc. Nat. Acad. Sci. USA* **85**, 3643-3647.

Neer, E. J. and Clapham, D. E. (1988). Roles of G protein subunits in transmembrane signalling. *Nature* **333**, 129-134.

Nicholson, G. C., Livesey, S. A., Moseley, J. M. and Martin, T. J. (1986). Actions of calcitonin, parathyroid hormone, and prostaglandin E_2 on cyclic AMP formation in chicken and rat osteoclasts. *J. Cell. Biochem.* **31**, 229-241.

Oberhauser, A. F., Monck, J. R., Balch, W. E. and Fernandez, J. M. (1992). Exocytotic fusion is activated by Rab3a peptides. *Nature* **360**, 270-273.

Ohmori, H., Toyama, S. and Toyama, S. (1992). Direct proof that the primary site of action of cytochalasin on cell motility processes is actin. *J. Cell Biol.* **116**, 933-941.

Ridley, A. J. and Hall, A. (1992). The small GTP-binding protein rho regulates the assembly of focal adhesions and actin stress fibers in response to growth factors. *Cell* **70**, 389-399.

Ridley, A. J., Paterson, H. F., Johnston, C. L., Diekmann, D. and Hall, A. (1992). The small GTP-binding protein rac regulates growth factor-induced membrane ruffling. *Cell* **70**, 401-410.

Sims, S. M. and Dixon, S. J. (1989). Inwardly rectifying K^+ current in osteoclasts. *Amer. J. Physiol.* **256**, C1277-C1282.

Sims, S. M., Kelly, M. E. M. and Dixon, S. J. (1991). K^+ and Cl^- currents in freshly isolated rat osteoclasts. *Pflügers Arch.* **419**, 358-370.

Smith, S. J. (1988). Neuronal cytomechanics: the actin-based motility of growth cones. *Science* **242**, 708-715.

Teti, A., Colucci, S., Grano, M., Argentino, L. and Zambonin-Zallone, A. (1992). Protein kinase C affects microfilaments, bone resorption, and $[Ca^{2+}]$ sensing in cultured osteoclasts. *Amer. J. Physiol.* **263**, C130-C139.

Therrien, S. and Naccache, P. H. (1989). Guanine nucleotide-induced polymerization of actin in electropermeabilized human neutrophils. *J. Cell Biol.* **109**, 1125-1132.

Turksen, K., Kanehisa, J., Opas, M., Heersche, J. N. M. and Aubin, J. E. (1988). Adhesion patterns and cytoskeleton of rabbit osteoclasts on bone slices and glass. *J. Bone Miner. Res.* **3**, 389-400.

Ui, M. (1990). Pertussis toxin as a valuable probe for G-protein involvement in signal transduction. In *ADP-Ribosylating Toxins and G Proteins. Insights into Signal Transduction* (ed. J. Moss and M. Vaughan), pp. 45-77. American Society for Microbiology Press, Washington, DC.

Venable, M. E., Zimmerman, G. A., McIntyre, T. M. and Prescott, S. M. (1993). Platelet-activating factor: a phospholipid autacoid with diverse actions. *J. Lipid Res.* **34**, 691-702.

Wood, D. A., Hapak, L. K., Sims, S. M. and Dixon, S. J. (1991). Direct effects of platelet-activating factor on isolated rat osteoclasts: rapid elevation of intracellular free calcium and transient retraction of pseudopods. *J. Biol. Chem.* **266**, 15369-15376.

Yatani, A., Codina, J. and Brown, A. M. (1990). G protein-mediated effects on ionic channels. In *G Proteins* (ed. R. Iyengar and L. Birnbaumer), pp. 241-266. Academic Press, Inc., San Diego, CA.

Zaidi, M., Datta, H. K., Moonga, B. S. and MacIntyre, I. (1990). Evidence that the action of calcitonin on rat osteoclasts is mediated by two G proteins acting via separate post-receptor pathways. *J. Endocrinol.* **126**, 473-481.

Zheng, Z. G., Wood, D. A., Sims, S. M. and Dixon, S. J. (1993). Platelet-activating factor stimulates resorption by rabbit osteoclasts in vitro. *Amer. J. Physiol.* **264**, E74-E81.

Zimmermann, A., Gehr, P. and Keller, H. U. (1988). Diacylglycerol-induced shape changes, movements and altered F-actin distribution in human neutrophils. *J. Cell Sci.* **90**, 657-666.

(Received 21 June 1993 - Accepted, in revised form, 19 October 1993)